

Analysis of Clock Jitter in Continuous-Time Sigma-Delta Modulators

V.Vasudevan, *Member, IEEE*

Abstract—One of the factors limiting the performance of continuous-time sigma-delta modulators (CTSDM) is clock jitter. This jitter can be classified as synchronous and accumulated/long-term jitter. A clock that is derived from a phase-lock loop (PLL) contains both types of jitter. In this paper, we present a framework that can be used to obtain the output spectrum in the presence of jitter, either synchronous or accumulated, or a combination of both. First, a general expression for the output power spectral density of the CTSDM in the presence of clock jitter is derived. Based on this, analytical expressions for the output power spectral density are obtained for particular cases of synchronous and long-term jitter. These are validated against behavioural simulations.

Index Terms—Clock jitter, sigma-delta modulator

I. INTRODUCTION

The continuous-time sigma-delta-modulator (CTSDM) has received a lot of attention recently due to its potential for obtaining high resolutions at low operating power. One problem limiting its performance is clock jitter. This jitter can be classified as synchronous and long-term (accumulated) jitter [1]. An analysis of jitter in phase-lock loops (PLL) indicates that the jitter in the output is a combination of correlated synchronous and long-term jitter [2], [1]. In the literature, the effect of white synchronous jitter on CTSDMs has been analyzed extensively [3], [4], [5], [6]. Recently, the effect of synchronous correlated jitter has been studied in [7]. In both cases, jitter is treated as a perturbation, which is possible because the variance of jitter is bounded. There has been no systematic study of the effects of accumulated jitter, although there is an empirical expression given in [3]. Perturbation models cannot be used in the case of long-term jitter since its variance is unbounded.

In this paper, we develop a general theory for the analysis of the effects of clock jitter in CTSDMs, using nonlinear models for jitter. Since nonlinear jitter models are used, both synchronous and long-term jitter can be analyzed using a common framework. We first derive a general expression for the output power spectral density (PSD) of the CTSDM in the presence of clock jitter. Based on this, we obtain analytical expressions for the output PSD for particular cases of synchronous and long-term jitter. For the case of white synchronous jitter, we show that the expression for the output PSD is a slightly more accurate version of the commonly used approximation. For correlated synchronous and long-term jitter, we derive analytical expressions for the output PSD that match very well with simulations using behavioural models. Using this framework, it is also possible to obtain the output spectrum if the clock has a combination of synchronous and

long-term jitter. As a part of this analysis, we also obtain expressions for the effect of timing jitter on digital to analog converters (DACs). Throughout the analysis, we assume a non-return-to-zero DAC, which is usually the DAC used in CTSDMs, since it has better performance than the return-to-zero DAC in presence of clock jitter.

The paper is organized as follows. Section II describes the model and some of the assumptions used in the analysis. In section III, we derive expressions for the output PSD of the DAC in the presence of clock jitter. This is followed by an analysis of the modulator in section IV. In section V, we derive expressions for the output PSD in the presence of various types of jitter. Section VI contains comparisons with behavioural simulations and a discussion of the results. Section VII concludes the paper.

II. MODEL

Figure 1(a) shows the model that is typically used to analyze a CTSDM with clock jitter. Clock jitter affects both the quantizer and the feedback DAC. However, within the signal band, since the loop gain is large, jitter in the quantizer has a negligible effect on the output spectrum. As a result, jitter induced errors within the signal band of the output spectrum occur mainly due to the feedback DAC. In Figure 1(a), $y_d^{(j)}[n]$ is the output digital signal and $g_c(t)$ is the DAC output. With no clock jitter, $g_c(t) = y_d^j(t)$, which is the continuous-time version of $y_d^j[n]$. With clock jitter, $g_c(t) = y_d^j(t + \xi(t))$, where $\xi(t)$ is a random process that models the jitter. For typical oversampling ratios (OSRs), the modulator can be analyzed as a discrete-time system. Therefore, sampled versions of $x_c(t)$ ($x_d[n]$) and $g_c(t)$ ($g_d[n]$) are used and the loop filter is modelled as a discrete-time filter. For purposes of analysis, usually a linear model of the analog-to-digital converter (ADC) is used, where the quantization error $q[n]$, is modelled as uniformly distributed additive white noise.

In the literature, jitter is treated as a perturbation to the ideal and the feedback signal $g_d[n]$ can be written as

$$\begin{aligned} g_d[n] &= y_d^{(i)}[n] + \frac{\xi[n]}{T} \left(y_d^{(i)}[n] - y_d^{(i)}[n-1] \right) \\ &= y_d^{(i)}[n] + j[n] \end{aligned} \quad (1)$$

Here, $y_d^{(i)}[n]$ is the output of an ideal modulator (i.e, a modulator with no clock jitter), $j[n]$ is the voltage error corresponding to the timing error $\xi[n]$ and T is the clock period. The negative feedback loop compensates for this error in the feedback signal at the input, resulting in a non-ideal output spectrum. Since the jitter-induced error is modelled as

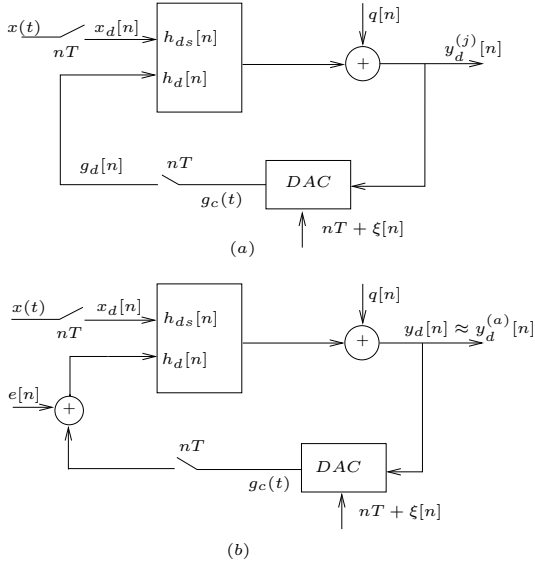


Fig. 1. Discrete-time linearized model of the modulator with clock jitter (a) Actual modulator and (b) A fictitious modulator with an independent process $e[n]$ added to the DAC output

an additive error at the input, the actual output spectrum is the sum of the ideal spectrum and this error (multiplied by an appropriate transfer function), i.e.,

$$S_{y_d}^{(j)}(e^{j\omega T}) = S_{y_d}^{(i)}(e^{j\omega T}) + S_j(e^{j\omega T}) \frac{|H_d(e^{j\omega T})|^2}{|1 + H_d(e^{j\omega T})|^2} \quad (2)$$

Here, $S_{y_d}^{(j)}(e^{j\omega T})$ is the output PSD of a modulator with jitter, $S_{y_d}^{(i)}(e^{j\omega T})$ is the PSD at the output of an ideal modulator, $S_j(e^{j\omega T})$ is the PSD of the voltage error $j[n]$ and $H_d(e^{j\omega T})$ is the discrete-time transfer function of the loop filter. The assumption here is that the error due to jitter appears as an additive error and the error due to jitter $j[n]$ is independent of the output voltage.

An equivalent way to look at this model is as shown in Figure 1(b). It is a fictitious modulator in which we add an independent random process $e[n]$ in an attempt to compensate for the error in the feedback signal. This is essentially the same error that the negative feedback loop tries to compensate, which then appears at the output of the real modulator. If the jitter is truly additive and the compensation is exact, then the output PSD of the modulator will be close to the ideal output.

The loop equation for this fictitious modulator can be written as

$$y_d[n] + (g_d * h_d)[n] = (x * h_{ds})[n] + q[n] - (e * h_d)[n] \quad (3)$$

In the equation, $*$ represents the convolution operator, $h_d[n]$ is the impulse response of the feedback path in the loop filter and $h_{ds}[n]$ is the impulse response of the signal path. We need to solve for the PSD of the output, $y_d[n]$, denoted by $S_{y_d}(e^{j\omega T})$. If $g_d[n]$ is given by equation (1), the loop equation in terms of the power spectral densities can be written as:

$$S_{y_d}(e^{j\omega T}) + S_j(e^{j\omega T})|JTF|^2 = S_{x_d}(e^{j\omega T})|STF|^2 + S_q(e^{j\omega T})|NTF|^2 + S_e(e^{j\omega T})|JTF|^2 \quad (4)$$

where

$$\begin{aligned} |STF|^2 &= \frac{|H_{ds}(e^{j\omega T})|^2}{|1 + H_d(e^{j\omega T})|^2} \\ |NTF|^2 &= \frac{1}{|1 + H_d(e^{j\omega T})|^2} \\ |JTF|^2 &= \frac{|H_d(e^{j\omega T})|^2}{|1 + H_d(e^{j\omega T})|^2} \end{aligned} \quad (5)$$

Here $S_{x_d}(e^{j\omega T})$, $S_q(e^{j\omega T})$ and $S_e(e^{j\omega T})$ are the PSDs of the input $x_d[n]$, the quantization error $q[n]$ and the random process $e[n]$. $H_d(e^{j\omega T})$ and $H_{ds}(e^{j\omega T})$ are the Fourier transforms of the two impulse responses $h_d[n]$ and $h_{ds}[n]$. STF , NTF and JTF denote the signal, noise and the jitter transfer functions.

An approximate solution to the loop equation is given by

$$\begin{aligned} S_{y_d}(e^{j\omega T}) &\approx S_{y_d}^{(a)}(e^{j\omega T}) \\ &= S_{x_d}(e^{j\omega T})|STF|^2 + S_q(e^{j\omega T})|NTF|^2 \\ &= S_{y_d}^{(i)}(e^{j\omega T}) \\ S_e(e^{j\omega T}) &= S_j(e^{j\omega T}) \end{aligned} \quad (6)$$

In the above equation, $S_j(e^{j\omega T})$ can be obtained from equation (1) [3], [4]. This is an approximate solution, since in general, $S_j(e^{j\omega T})$ is a function of $S_{y_d}(e^{j\omega T})$. To compute $S_j(e^{j\omega T})$, $S_{y_d}^{(a)}(e^{j\omega T})$ is used (which in this case is the ideal output spectrum). In the real modulator, the negative feedback loop will try to compensate for $S_j(e^{j\omega T})$ at the input resulting in an output spectral density given by:

$$S_{y_d}^{(j)}(e^{j\omega T}) \approx S_{y_d}^{(a)}(e^{j\omega T}) + S_e(e^{j\omega T})|JTF|^2 \quad (7)$$

where $S_{y_d}^{(a)}(e^{j\omega T})$ and $S_e(e^{j\omega T})$ are given in equation (6).

The results using an ‘‘additive jitter error’’ model are found to match reasonably well with behavioural simulations and with experiment. Therefore, in this paper, we continue to use this model. However, we obtain more accurate expressions for $S_{y_d}^{(a)}(e^{j\omega T})$ and $S_e(e^{j\omega T})$ based on a more accurate nonlinear jitter model. For various types of jitter, we write the loop equation in a form similar to equation (4) and find expressions for $S_{y_d}^{(a)}(e^{j\omega T})$ and $S_e(e^{j\omega T})$. These are then used to find the output PSD using equation (7).

The first step towards analysis of the modulator is to get an expression for the output of the feedback DAC in the presence of clock jitter. This is done in the next section.

III. ANALYSIS OF THE DAC

In this section, we obtain the PSD of the DAC output signal in the presence of clock jitter. The analysis in this section is based on work reported in [8]. The input to the DAC is a uniformly spaced discrete-time signal, $y_d[n]$. Its PSD can be written as

$$S_{y_d}(e^{j\omega T}) = \frac{1}{f_s} \sum_k R_{y_d}[k] e^{-jk\omega T} \quad (8)$$

In the above equation, $R_{y_d}[k]$ is the autocorrelation of the output signal, T is the clock period and f_s is the clock frequency. In terms of the unit step function $u(t)$, the continuous-time signal $y_c(t)$ corresponding to $y_d[k]$ can be written as:

$$y_c(t) = \sum_k y_d[k] (u(t - kT) - u(t - (k + 1)T)) \quad (9)$$

The power spectral density of $y_c(t)$, $S_{y_c}(\omega)$, is given by:

$$S_{y_c}(\omega) = \frac{|1 - e^{-j\omega T}|^2}{(\omega T)^2} S_{y_d}(e^{j\omega T}) \quad (10)$$

This is the spectrum of the signal at the output of the DAC if the clock were jitter free. However, if the clock has jitter, the output of the DAC is the time-distorted version of $y_c(t)$, denoted by $g_c(t)$. Let the clock jitter be denoted by $\xi(t)$. The autocorrelation of the jittered waveform, $R_{g_c}(t, \tau)$, can be written as:

$$\begin{aligned} R_{g_c}(t, \tau) &= E\{g_c(t + \tau)g_c(t)\} \\ &= E_{\xi}\{R_{y_c}(\tau + \xi(t + \tau) - \xi(t))\} \end{aligned} \quad (11)$$

$E_{\xi}(\cdot)$ is the expectation with respect to ξ and $R_{y_c}(t)$ is the autocorrelation of $y_c(t)$ conditional to ξ . If $\alpha(t, \tau) = \xi(t + \tau) - \xi(t)$ and $f(\alpha(t, \tau), \tau)$ is the probability density function of $\alpha(t, \tau)$, we have

$$R_{g_c}(t, t + \tau) = \int_{-\infty}^{\infty} R_{y_c}(\tau + \alpha(t, \tau))f(\alpha(t, \tau), \tau)d\alpha \quad (12)$$

In terms of $S_{y_c}(\omega)$, this autocorrelation can be written as:

$$R_{g_c}(t, t + \tau) = \frac{1}{2\pi} \iint_{-\infty}^{\infty} S_{y_c}(\eta)f(\alpha(t, \tau), \tau)e^{j\eta(\tau + \alpha(t, \tau))}d\eta d\alpha \quad (13)$$

Now, the characteristic function $M(\eta, \tau, t)$ of $\alpha(t, \tau)$ is given by:

$$M(\eta, \tau, t) = E\{e^{j\eta\alpha(t, \tau)}\} = \int_{-\infty}^{\infty} f(\alpha(t, \tau), \tau)e^{j\eta\alpha(t, \tau)}d\alpha \quad (14)$$

Substituting for this in equation (13), we get

$$R_{g_c}(t, t + \tau) = \frac{1}{2\pi} \int_{-\infty}^{\infty} S_{y_c}(\eta)M(\eta, \tau, t)e^{j\eta\tau}d\eta \quad (15)$$

The power spectral density of $g_c(t)$, $S_{g_c}(\omega, t)$ can be obtained as the Fourier transform of the autocorrelation function. It is given by

$$S_{g_c}(\omega, t) = \frac{1}{2\pi} \int_{-\infty}^{\infty} S_{y_c}(\eta)Q_c(\eta, \omega - \eta, t)d\eta \quad (16)$$

where

$$Q_c(\eta, \omega - \eta, t) = \int_{-\infty}^{\infty} M(\eta, \tau, t)e^{-j(\omega - \eta)\tau}d\tau \quad (17)$$

$Q_c(\eta, \omega - \eta, t)$ is the Fourier transform of the characteristic function $M(\eta, \tau, t)$ evaluated at $\omega - \eta$. It can be evaluated for various types of jitter as shown in the following subsections.

A. Synchronous white jitter

This cannot be evaluated for the DAC alone, since continuous time white noise does not exist. However, as will be seen later, it is not an issue when the DAC is used within the modulator, since we use a discrete time model for the modulator.

B. Synchronous correlated jitter

Here we assume that $\xi(t)$ is a correlated Gaussian process with autocorrelation given by

$$R_{\xi}(\tau) = \sigma^2 e^{-a|\tau|} \quad (18)$$

σ^2 is the variance of $\xi(t)$ and a is a measure of the correlation. The expression represents a simple first order correlation. This form for the autocorrelation is motivated by the autocorrelation of jitter in the PLL [2]. Using this, the variance of $\alpha(t, \tau)$, σ_{α}^2 , can be written as:

$$\sigma_{\alpha}^2 = 2\sigma^2(1 - e^{-a|\tau|}) \quad (19)$$

Therefore, characteristic function of $\alpha(\tau)$ is given by

$$\begin{aligned} M(\eta, \tau, t) &= e^{-\frac{\eta^2 \sigma_{\alpha}^2}{2}} \\ &= e^{-\eta^2 \sigma^2} \sum_{l=0}^{\infty} \frac{(\eta^2 \sigma^2)^l}{l!} e^{-la|\tau|} \end{aligned} \quad (20)$$

The Fourier transform of the characteristic function is thus

$$Q_c(\eta, \omega - \eta) = e^{-\eta^2 \sigma^2} \sum_{l=0}^{\infty} \frac{(\eta^2 \sigma^2)^l}{l!} \frac{2la}{(la)^2 + (\omega - \eta)^2} \quad (21)$$

C. Long term jitter

In this case, $\xi(t)$ is a random walk process. The characteristic function of $\alpha(t, \tau)$ is given by

$$M(\eta, \tau, t) = e^{-\frac{\eta^2 c |\tau|}{2}} \quad (22)$$

where c is the ‘‘diffusion coefficient’’ of the jitter. The Fourier transform of the characteristic function can be written as

$$Q_c(\eta, \omega - \eta) = \frac{\eta^2 c}{(\frac{\eta^2 c}{2})^2 + (\omega - \eta)^2} \quad (23)$$

IV. ANALYSIS OF THE MODULATOR

Since the modulator is analyzed as a discrete-time system, we need a sampled version of the autocorrelation of the DAC output signal, $R_{g_d}[n, n + k]$. It can be obtained from equation (15) as

$$R_{g_d}[n, n + k] = \frac{1}{2\pi} \int_{-\infty}^{\infty} S_{y_c}(\eta)M(\eta, kT, nT)e^{j\eta kT}d\eta \quad (24)$$

This can equivalently be written as

$$\begin{aligned} R_{g_d}[n, n + k] &= \frac{1}{2\pi} \sum_m \int_{-\pi f_s}^{\pi f_s} S_{y_c}(\eta - m\omega_s) \\ &\quad M(\eta - m\omega_s, kT, nT)e^{j\eta kT}d\eta \end{aligned} \quad (25)$$

The corresponding PSD, $S_{g_d}(e^{j\omega T})$, is therefore

$$\begin{aligned} S_{g_d}(e^{j\omega T}) &= \frac{1}{2\pi f_s} \sum_m \int_{-\pi f_s}^{\pi f_s} S_{y_c}(\eta - m\omega_s) \\ &\quad Q_d(\eta - m\omega_s, \omega - \eta, nT)d\eta \end{aligned} \quad (26)$$

where

$$Q_d(\eta - m\omega_s, \omega - \eta, nT) = \sum_k M(\eta - m\omega_s, kT, nT) e^{-j(\omega - \eta)kT} \quad (27)$$

It is the discrete Fourier transform of the sampled characteristic function.

As explained in section II, we first analyze a modulator that has an independent process $e[n]$ added to the output of the DAC. The loop equation of this modulator is given by equation (3). In terms of PSDs, this loop equation can be written as:

$$S_{y_d}(e^{j\omega T}) + S_{g_d}(e^{j\omega T})|H_d(e^{j\omega T})|^2 + S_{y_d g_d}(e^{j\omega T})H_d^*(e^{j\omega T}) + S_{g_d y_d}(e^{j\omega T})H_d(e^{j\omega T}) = S_{x_d}(e^{j\omega T})|H_{ds}(e^{j\omega T})|^2 + S_q(e^{j\omega T}) + S_e(e^{j\omega T})|H_d(e^{j\omega T})|^2 \quad (28)$$

$S_{y_d g_d}(e^{j\omega T})$ is the cross-spectral density between the output and the feedback signal. As mentioned, the aim is to put the above equation in a form similar to equation (4). We can then obtain expressions for $S_{y_d}^{(a)}(e^{j\omega T})$ and $S_e(e^{j\omega T})$ and use them to find the output PSD of the real modulator.

Equation (28) indicates that to find the output power spectral density, we need to find the cross-spectral density. To do this, we first compute the cross-correlation terms $R_{y_d g_d}[n, k]$ by sampling the corresponding continuous-time cross-correlation $R_{y_c g_c}(t, t + \tau)$. Now,

$$R_{y_c g_c}(t, t + \tau) = E\{y_c(t + \tau)g_c^*(t)\} = E_{\xi}\{R_{y_c}(\tau + \xi(t))\} \quad (29)$$

Since the autocorrelation $R_{y_c}(t)$ can be written as the inverse transform of the power spectral density, we have

$$R_{y_c g_c}(t, t + \tau) = \frac{1}{2\pi} \int_{-\infty}^{\infty} S_{y_c}(\eta) E_{\xi}\{e^{j\eta\xi(t)}\} e^{j\eta\tau} d\eta \quad (30)$$

The sampled cross-correlation can therefore be written as

$$R_{y_d g_d}[n, n + k] = \frac{1}{2\pi} \sum_m \int_{-\pi f_s}^{\pi f_s} S_{y_c}(\eta - m\omega_s) E_{\xi}\{e^{j(\eta - m\omega_s)\xi(nT)}\} e^{j\eta kT} d\eta \quad (31)$$

The corresponding cross-spectral density is given by:

$$S_{y_d g_d}(e^{j\omega T}, nT) = \frac{1}{2\pi f_s} \sum_m \int_{-\pi f_s}^{\pi f_s} S_{y_c}(\eta - m\omega_s) E_{\xi}\{e^{j(\eta - m\omega_s)\xi(nT)}\} \left(\sum_k e^{-j(\omega - \eta)kT} \right) d\eta \quad (32)$$

$R_{g_d y_d}[n, n + k]$ and $S_{g_d y_d}(e^{j\omega T}, nT)$ can be found in a similar manner. This analysis indicates that to find the power spectral density of the jittered waveform, we need to first find the Fourier transform of the sampled characteristic function of jitter. This can then be used to obtain an expression for $S_{g_d}(e^{j\omega T})$ using equation (26). We also need to evaluate the cross-spectral densities for various types of jitter. This is done in the following subsections.

A. White synchronous jitter

In this case, jitter is regarded as a perturbation with uncorrelated timing errors. Therefore, the characteristic function can be written as:

$$M(\eta - m\omega_s, kT, nT) = e^{-(\eta - m\omega_s)^2 \sigma^2}, \quad k \neq 0 \\ = 1, \quad k = 0 \quad (33)$$

σ^2 is the variance of the clock jitter. Note that the characteristic function is independent of n . The discrete Fourier transform of this function at $\omega - \eta$ is obtained as:

$$Q_d(\eta - m\omega_s, \omega - \eta) = (2\pi f_s) e^{-(\eta - m\omega_s)^2 \sigma^2} \delta(\omega - \eta) + (1 - e^{-(\eta - m\omega_s)^2 \sigma^2}) \quad (34)$$

Substituting this in equation (26), we get

$$S_{g_d}(e^{j\omega T}) = \sum_m e^{-(\omega - m\omega_s)^2 \sigma^2} S_{y_c}(\omega - m\omega_s) + \sum_m \frac{1}{2\pi f_s} \int_{-\pi f_s}^{\pi f_s} S_{y_c}(\eta - m\omega_s) \left(1 - e^{-(\eta - m\omega_s)^2 \sigma^2}\right) d\eta \quad (35)$$

Now, the first term in the above equation can be written as:

$$S_{y_d}(e^{j\omega T}) \sum_m e^{-(\omega - m\omega_s)^2 \sigma^2} \text{sinc}^2((\omega - m\omega_s)T/2) \quad (36)$$

This expression can be used directly in the equation (28) and the resulting loop equation can be solved to obtain an expression for $S_{y_d}^{(a)}(e^{j\omega T})$. The disadvantage of doing this is that the series sum has to be evaluated for each jitter variance. Instead, we can get a very good approximation by noting that, for all practical values of jitter, the exponential term is close to one and it dies down more slowly than the ‘‘sinc’’ function. Therefore, to a very good approximation, its effects on aliasing can be ignored and the term (36) can be approximated as:

$$e^{-\omega^2 \sigma^2} S_{y_d}(e^{j\omega T}) \sum_m \text{sinc}^2((\omega - m\omega_s)T/2) \quad (37)$$

With m in the range ± 20 and 1% jitter, the error due to this approximation is only about 0.6% at $f_s/2$ and is smaller at lower frequencies. If there is 5% jitter, the error in this approximation is about 6% at $f_s/2$. We can make similar approximations for the second term. Denoting the series sum of ‘‘sinc squared’’ functions as $S(\omega)$, the second term in equation (35) can be approximated as:

$$\frac{1}{2\pi f_s} \int_{-\pi f_s}^{\pi f_s} S(\eta) S_{y_d}(e^{j\eta T}) \left(1 - e^{-\eta^2 \sigma^2}\right) d\eta \quad (38)$$

The resulting error in the signal-to-noise ratio (SNR) depends on the shape and the high frequency gain of the NTF. However, in all the cases simulated, this approximation gives an SNR to within 0.2 – 0.3dB of the simulated value, with four aliasing sidebands ($-4 \leq m \leq 4$). With only one sideband included, the SNR matches to within 1dB. If the range of m is increased to a very large value, the approximation will overestimate the amount of aliasing, but the SNR remains within 0.5dB of the

simulated value. This is true even for 10% clock jitter where the error in the approximation is larger.

In order to obtain the cross-correlation, we need to find $E_{\xi}\{e^{j\eta\xi(nT)}\}$ and $E_{\xi}\{e^{j\eta\xi((n+k)T)}\}$. In this case, both are equal to $e^{-\eta^2\sigma^2/2}$. Making similar approximations as for $S_{gd}(e^{j\omega T})$, the expressions for the cross-spectral densities are given by:

$$S_{y_d g_d}(e^{j\omega T}) = S_{g_d y_d}(e^{j\omega T}) \approx e^{-\omega^2\sigma^2/2} S_{y_d}(e^{j\omega T}) S(\omega) \quad (39)$$

B. Correlated synchronous jitter

In this case, jitter is regarded as a perturbation, but the timing errors are correlated. Here, we assume an autocorrelation of the form given in equation (18). In this case, the characteristic function can be written as:

$$M(\eta - m\omega_s, kT) = e^{-(\eta - m\omega_s)^2\sigma^2(1 - e^{-a|k|T})}$$

As in the case of white synchronous jitter, the value of $M(\eta, kT)$ is close to one up to $\omega_s/2$ and dies down slowly after that. Therefore, we can make similar approximations as for the white synchronous jitter case and $S_{gd}(e^{j\omega T})$ can be written as:

$$S_{gd}(e^{j\omega T}) \approx \frac{1}{2\pi f_s} \int_{-\pi f_s}^{\pi f_s} S(\eta) S_{y_d}(e^{j\eta T}) Q_d(\eta, \omega - \eta) d\eta \quad (40)$$

where

$$Q_d(\eta, \omega - \eta) = e^{-\eta^2\sigma^2} \sum_{l=0}^{\infty} \frac{(\eta^2\sigma^2)^l}{l!} \left[\frac{1 - e^{-2laT}}{1 + e^{-2laT} - 2e^{-laT} \cos((\omega - \eta)/f_s)} \right] \quad (41)$$

The error in the approximation is larger for larger values of a (relatively uncorrelated jitter). The upper bound for this error is the error incurred with white synchronous jitter.

If substituted directly in the loop equation (equation (28)), it becomes difficult to obtain even the approximate solution $S_{y_d}^{(a)}(e^{j\omega T})$. As mentioned previously, the aim is to write the loop equation in the form of equation (4), i.e. in a form suitable to the additive jitter model. To that end, we write this integral as a discrete sum over frequency bins of width Δf_i . Obviously, as the bin size becomes smaller, the integral is represented more accurately. The bin width needed to get good estimates of the SNR depends on the OSR and the shape of the NTF, but typically we have found that around hundred bins within the signal bandwidth is sufficient. A similar number of bins is required to get estimates of the SNR from behavioural simulations.

The main problem in writing it as a discrete sum is that $Q_d(\eta, \omega - \eta)$ has a peak at $\eta = \omega$ and falls very rapidly on both sides, especially for small values of a (large correlation times). Since $\eta^2\sigma^2$ is typically very small in the signal bandwidth, this maximum value can become very large. So, numerical estimation in a finite bin size becomes difficult. However, since the jitter power contained in a bin is limited, a numerically more robust estimate can be obtained by finding

the approximate jitter power in each bin. On doing this, we obtain

$$S_{gd}(e^{j\omega T}) \approx \sum_i S(f_i) S_{y_d}(f_i) e^{-(2\pi f_i \sigma)^2} \times \sum_{l=0}^{\infty} \frac{((2\pi f_i)^2 \sigma^2)^l}{l!} P_f^c(f_i) \quad (42)$$

where $P_f^c(f_i)$ is the jitter power in each frequency bin and is given by

$$P_f^c(f_i) = \int_{f_i - \frac{\Delta f_i}{2}}^{f_i + \frac{\Delta f_i}{2}} \frac{1 - e^{-2laT}}{1 + e^{-2laT} - 2e^{-laT} \cos(2\pi(f - \nu)/f_s)} \frac{d\nu}{f_s} \quad (43)$$

It is possible to obtain an analytical expression for the above integral [9] and it is given by

$$P_f^c(f_i) = 0, \quad l = 0, f_i \neq f \\ = \frac{1}{\pi} \left[\tan^{-1} \left\{ \frac{1+A}{1-A} \tan \left(\frac{\pi(f - f_i + 0.5\Delta f_i)}{f_s} \right) \right\} \right. \\ \left. - \tan^{-1} \left\{ \frac{1+A}{1-A} \tan \left(\frac{\pi(f - f_i - 0.5\Delta f_i)}{f_s} \right) \right\} \right], \text{ elsewhere} \quad (44)$$

where $A = e^{-laT}$. The discrete sum can then be written as a sum of two components, namely, the PSD at $f = \frac{\omega}{2\pi}$, where spectrum is desired, and the sum of the PSDs at the other frequencies. Therefore,

$$S_{gd}(e^{j\omega T}) \approx S(f) S_{y_d}(f) e^{-(2\pi f \sigma)^2} \sum_{l=0}^{\infty} \frac{((2\pi f)^2 \sigma^2)^l}{l!} P_f^c(f) \\ + \sum_{f_i \neq f} S(f_i) S_{y_d}(f_i) e^{-(2\pi f_i \sigma)^2} \sum_{l=1}^{\infty} \frac{((2\pi f_i)^2 \sigma^2)^l}{l!} P_f^c(f_i) \quad (45)$$

Since $E_{\xi}\{e^{j\eta\xi(nT)}\}$ and $E_{\xi}\{e^{j\eta\xi((n+k)T)}\}$ are both equal to $e^{-\eta^2\sigma^2/2}$, the cross-spectral densities are given by equation (39)

C. Long-term jitter

The discrete time version of the characteristic function given by equation (22) can be written as

$$M(\eta - m\omega_s, kT, nT) = e^{-\frac{|k|(\eta - m\omega_s)^2\sigma^2}{2}} \quad (46)$$

In the above equation, $\sigma^2 = cT$. In this case, it is not possible to make the same approximations as for the previous two cases. The discrete Fourier transform of $M(\eta, kT)$ is given by:

$$Q_d(\eta, \omega - \eta) = \frac{1 - e^{-\eta^2\sigma^2}}{1 + e^{-\eta^2\sigma^2} - 2e^{-\frac{\eta^2\sigma^2}{2}} \cos((\omega - \eta)/f_s)} \quad (47)$$

In this case, we can write $S_{g_d}(e^{j\omega T})$ as

$$S_{g_d}(e^{j\omega T}) = \frac{1}{2\pi f_s} \int_{-\pi f_s}^{\pi f_s} \sum_m S_{y_c}(\eta - m\omega_s) Q_d(\eta - m\omega_s, \omega - \eta) d\eta \quad (48)$$

The function $Q_d(\eta, \omega - \eta)$ has a relatively narrow peak at $\eta = \omega$ and falls down quite rapidly on both sides. Since its effect is localized, aliasing from the other frequency bands is quite small. In all the simulations performed, we have seen that completely neglecting aliasing gives an error of about $1 - 2dB$ in the SNR. If one sideband is included, the error in the SNR is of the order of $0.3 - 0.5dB$.

As in the case of correlated jitter, we write the integral as a discrete sum. On doing this, we obtain

$$S_{g_d}(e^{j\omega T}) \approx S_{y_c}(f)P_f^l(f) + \sum_{f_i \neq f} S_{y_c}(f)P_f^l(f_i) \quad (49)$$

It is convenient in this case to expand the series sum, with the range of f_i depending on the number of aliasing frequency bands. $P_f^l(f_i)$ is the jitter power (due to long-term jitter) in the i^{th} frequency bin, given by:

$$\begin{aligned} P_f^l(f_i) &= \int_{f_i - \frac{\Delta f}{2}}^{f_i + \frac{\Delta f}{2}} \frac{1 - A_i^2}{1 + A_i^2 - 2A_i \cos(2\pi(f - \nu)/f_s)} \frac{d\nu}{f_s} \\ &= \frac{1}{\pi} \left[\tan^{-1} \left\{ \frac{1 + A_i}{1 - A_i} \tan \left(\frac{\pi(f - f_i + 0.5\Delta f_i)}{f_s} \right) \right\} \right. \\ &\quad \left. - \tan^{-1} \left\{ \frac{1 + A_i}{1 - A_i} \tan \left(\frac{\pi(f - f_i - 0.5\Delta f_i)}{f_s} \right) \right\} \right] \quad (50) \end{aligned}$$

Unlike the correlated jitter case, A_i is not a constant within the frequency bin. To obtain an analytical approximation for the integral, we assume A_i takes on the value at the midpoint of the bin. Hence $A_i = e^{-\frac{(2\pi f_i)^2 \sigma^2}{2}}$. This is a good approximation since the bin size is usually quite small. The number of bins used is similar to that in the previous case.

For long-term jitter, the asymptotic cross-correlations are given by

$$\lim_{n \rightarrow \infty} E_{\xi} \{ e^{j\eta \xi(nT)} \} = \lim_{n \rightarrow \infty} e^{-\eta^2 cnT} = 0 \quad (51)$$

Similarly, $E_{\xi} \{ e^{j\eta \xi([n+k]T)} \}$ also tends to zero asymptotically. This tells us that the correlation between the output signal and the jittered version of the output signal tends to zero. Although this result is a little counter-intuitive, it can be explained as follows. The continuous time version of the feedback signal is $g_c(t) = y_c(t + \xi(t))$. In the case of long-term jitter, the variance of $\xi(t)$ grows with time. When this happens, the sample paths of the feedback signal will be widely dispersed in time. Therefore, asymptotically, the ensemble average $E\{y_c(t)g_c^*(t + \tau)\}$ will go to zero. Consequently, the cross-spectral densities will also tend to zero. This is a consequence of the model that we use. As explained in section II, we neglect the effect of jitter errors due to the quantizer, since it is diminished by the loop gain. While this is a good approximation in the signal band,

it may not be as good an approximation at higher frequencies. So the quantizer output (or the modulator output) will not maintain perfect time as is assumed in the model, but will contain some high frequency jitter power. This in turn will lead to some correlation between the output and the feedback signal at higher frequencies. However, as mentioned, within the signal band, zero correlation is a very good approximation.

V. POWER SPECTRAL DENSITY OF THE OUTPUT SIGNAL OF THE MODULATOR

Using the results of the previous section, we obtain an equation for the output power spectral density for various types of jitter.

A. Synchronous white jitter

Using equations (35), (37), (38) and (39) in equation (28), we have

$$\begin{aligned} S_{y_d}(e^{j\omega T}) + S_j(e^{j\omega T}) \frac{|H_d(e^{j\omega T})|^2}{D} &= S_{x_d}(e^{j\omega T}) \\ \times \frac{|H_{ds}(e^{j\omega T})|^2}{D} + S_q(e^{j\omega T}) \frac{1}{D} + S_e(e^{j\omega T}) \frac{|H_d(e^{j\omega T})|^2}{D} &\quad (52) \end{aligned}$$

where D is given by

$$\begin{aligned} D &= 1 + S(\omega) \left[e^{-\omega^2 \sigma^2} |H_d(e^{j\omega T})|^2 \right. \\ &\quad \left. + e^{-\omega^2 \sigma^2 / 2} (H_d(e^{j\omega T}) + H_d^*(e^{j\omega T})) \right] \quad (53) \end{aligned}$$

and

$$S_j(e^{j\omega T}) = \frac{1}{2\pi f_s} \int_{-\pi f_s}^{\pi f_s} S(\eta) S_{y_d}(e^{j\eta T}) \left(1 - e^{-\eta^2 \sigma^2} \right) d\eta \quad (54)$$

Therefore, the approximate solution to the loop equation is

$$\begin{aligned} S_{y_d}^{(a)}(e^{j\omega T}) &= S_{x_d}(e^{j\omega T}) \frac{|H_{ds}(e^{j\omega T})|^2}{D} + S_q(e^{j\omega T}) \frac{1}{D} \\ S_e(e^{j\omega T}) &= \frac{1}{2\pi f_s} \int_{-\pi f_s}^{\pi f_s} S(\eta) S_{y_d}^{(a)}(e^{j\eta T}) \left(1 - e^{-\eta^2 \sigma^2} \right) d\eta \quad (55) \end{aligned}$$

As discussed in section II, the power spectral density at the output of the actual modulator is given by

$$S_{y_d}^{(j)}(e^{j\omega T}) = S_{y_d}^{(a)}(e^{j\omega T}) + S_e(e^{j\omega T}) \frac{|H_d(e^{j\omega T})|^2}{D} \quad (56)$$

In a sigma-delta converter, the sampling frequency is typically much larger than the signal bandwidth and σ is a fraction of the clock period. Therefore $\eta^2 \sigma^2$ is close to zero, giving

$$1 - e^{-\eta^2 \sigma^2} \approx \eta^2 \sigma^2 \quad (57)$$

Also, $e^{-\omega^2 \sigma^2}, S(\omega) \approx 1$, which means $D \approx |1 + H_d(e^{j\omega T})|^2$. In this case, $S_{y_d}^{(a)}(e^{j\omega T})$ is the same as the ideal output

spectrum, $S_{y_d}^{(i)}(e^{j\omega T})$. Further, if all aliasing from other frequency bands is neglected in the expression for $S_e(e^{j\omega T})$ i.e. $S(\eta) \approx \text{sinc}^2(\eta T/2)$, we get

$$S_e(e^{j\omega T}) = \frac{1}{2\pi f_s} \left(\frac{\sigma^2}{T^2} \right) \int_{-\pi f_s}^{\pi f_s} |1 - e^{-j\eta T}|^2 S_{y_d}^{(i)}(\eta) d\eta \quad (58)$$

This is the approximation that is commonly used in jitter calculations. It results in an error of about $1.5 - 2dB$ in the predicted SNR, which has also been reported [4].

B. Synchronous correlated jitter

Using equations (45) and (39) in the loop equation and following a procedure similar to the one used for synchronous white jitter, we can write approximate solution to the loop equation as:

$$\begin{aligned} S_{y_d}^{(a)}(e^{j\omega T}) &= S_{x_d}(e^{j\omega T}) \frac{|H_{ds}(e^{j\omega T})|^2}{D} + S_q(e^{j\omega T}) \frac{1}{D} \\ S_e(e^{j\omega T}) &\approx \sum_{f_i \neq f} S(f_i) S_{y_d}^{(a)}(f_i) e^{-(2\pi f_i \sigma)^2} \times \\ &\quad \sum_{l=0}^{\infty} \frac{((2\pi f_i)^2 \sigma^2)^l}{l!} P_f^c(f_i) \end{aligned} \quad (59)$$

where

$$\begin{aligned} D &= 1 + S(\omega) \left(e^{-\omega^2 \sigma^2} |H_d(e^{j\omega T})|^2 \times \right. \\ &\quad \left. \sum_{l=0}^{\infty} \frac{(\omega^2 \sigma^2)^l}{l!} P_f^c(f) + e^{-\omega^2 \sigma^2 / 2} [H_d(e^{j\omega T}) + H_d^*(e^{j\omega T})] \right) \end{aligned} \quad (60)$$

The output power spectral density of the actual modulator, $S_{y_d}^{(j)}(e^{j\omega T})$, can be computed using equation (56), using appropriate values for $S_{y_d}^{(a)}(e^{j\omega T})$ and $S_e(e^{j\omega T})$. In all the cases simulated, the SNR obtained using these expressions with four sidebands, are within $0.2 - 0.3dB$ of simulated values. As the correlation time increases i.e. a becomes smaller, the characteristic function is more nearly equal to one, as is assumed in the theory. In this case, the simulated and theoretical values of the SNR match to within $0.1dB$.

As for the case of white synchronous jitter, if $\omega^2 \sigma^2 \ll 1$, which is the case for typical OSRs, $S_{y_d}^{(a)}(e^{j\omega T})$ can be approximated well by the ideal output spectrum. A reasonable estimate of the SNR can be obtained by using the ideal spectrum and ignoring aliasing in the expression for $S_e(e^{j\omega T})$.

C. Long-term jitter

Using equation (49) and the fact that the cross-spectral densities are zero in the loop equation, an approximate solution to the loop equation can be written as:

$$\begin{aligned} S_{y_d}^{(a)}(e^{j\omega T}) &= \frac{|H_{ds}(e^{j\omega T})|^2}{D} S_{x_d}(e^{j\omega T}) + \frac{1}{D} S_q(e^{j\omega T}) \\ S_e(e^{j\omega T}) &\approx \sum_{f_i \neq f} \text{sinc}^2(\pi f_i T) S_{y_d}^{(a)}(f_i) P_f^l(f_i) \end{aligned} \quad (61)$$

where

$$D = 1 + |H_d(e^{j\omega T})|^2 \text{sinc}^2(\pi f T) P_f^l(f) \quad (62)$$

As mentioned, the range of f_i depends on the number of aliasing sidebands included. Once again, the output power spectral density can be computed using equation (56).

As a consequence of the zero correlation between the output and the feedback signal in this case, the random process $e[n]$ cannot compensate well for the errors due to jitter. Therefore, unlike the synchronous jitter case, $S_{y_d}^{(a)}(e^{j\omega T})$ cannot be approximated well by the ideal spectrum.

VI. RESULTS AND DISCUSSIONS

The results obtained using analytical expressions were compared with behavioural simulations for first, second and third order modulators. The second order modulator had a standard feedback architecture with $STF = z^{-1}$ and $NTF = (1 - z^{-1})^2$. The third order modulator was a feedforward modulator with a Butterworth loop filter. The out-of-band gain was 1.4. A time step of 0.5σ was used to integrate the state equations of the loop filter during behavioural simulations. Correlated random numbers were obtained using the method suggested in [10]. Results were obtained for a one-bit and two-bit quantizer as well as for a linear model with additive uniformly distributed quantization error. The output spectrum is the average power spectrum obtained from five simulations. A Hann window was used to find the discrete Fourier transform. The programs were written in Python and run on a Linux system. Some representative results are now discussed. All the results are plotted as a function of the normalized frequency (f/f_s).

A. White synchronous jitter

Figure 2 shows the results obtained for white synchronous jitter for two different signal amplitudes. The analytical model clearly predicts the noise due to jitter very well. The SNR matches to about $0.3dB$. As expected from the theory, noise level does not depend on the signal amplitude.

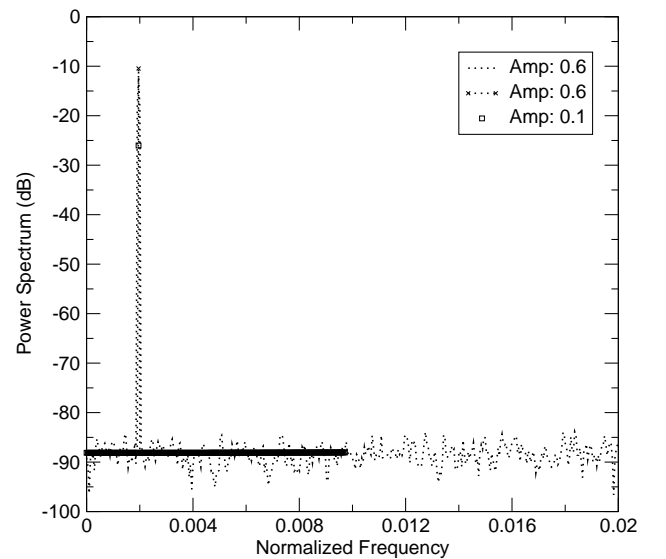


Fig. 2. Output spectrum of a second order modulator with an OSR of 128 and 1% white clock jitter. The quantizer is a two-bit quantizer.

B. Correlated synchronous jitter

Figure 3 shows a comparison of theoretical and simulation results for the case of correlated synchronous jitter, with two different jitter variances. The results are seen to match well. The difference between the theoretical and simulated values of the SNR is less than $0.1dB$, with four aliasing sidebands.

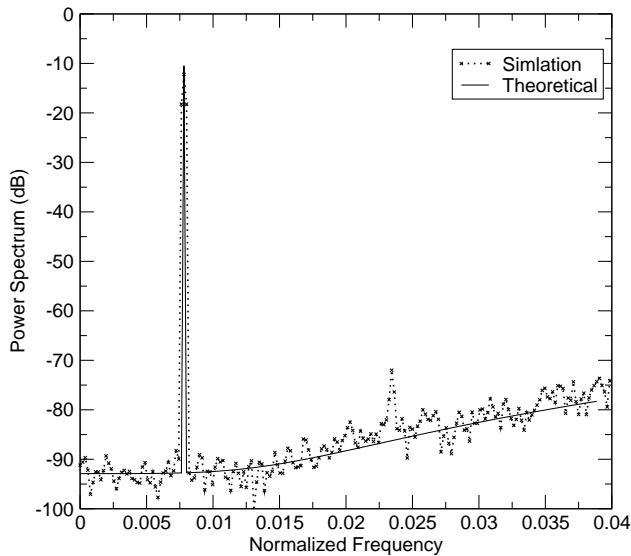


Fig. 3. Output spectrum of a second order modulator with an OSR of 32 and a correlation length of 10T with 1% clock jitter (signal amplitude is 0.6V). The quantizer is a two bit quantizer.

Figure (4) contains plots of the output spectrum for a fixed σ^2 and different correlation times. It is seen that the noise levels due to jitter are lower for longer correlation times. A similar trend is observed in Nyquist rate ADCs [11],[12].

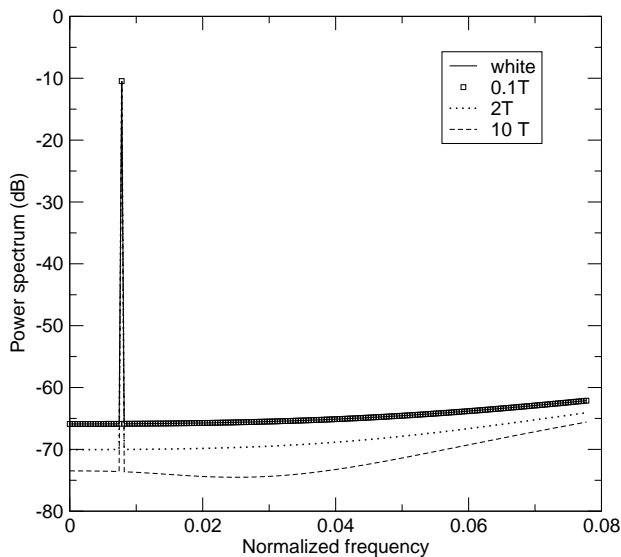


Fig. 4. Output spectrum of a second order modulator with an OSR of 32 and 10% jitter for various correlation times. The quantizer is a two bit quantizer.

In the case of synchronous jitter, the SNR obtained from simulations and analytical results matched very well (within $0.3dB$, usually better). As expected, the match is better for longer correlation times.

C. Long-term jitter

Figure 5 shows the results obtained for a third order modulator and an OSR of 128 with long-term clock jitter. Once again, the results of the analytical expressions match very well with behavioural simulations. It is seen from the figure that with long-term jitter, there is a spread in the signal spectrum at the output. Both this spread and the noise level due to jitter depend significantly on the signal amplitude.

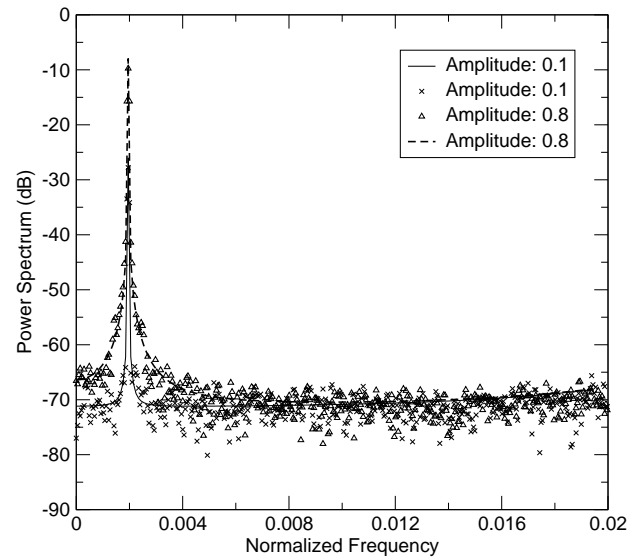


Fig. 5. Output spectrum of a third order modulator with an OSR of 128 and 10% long term clock jitter for two different input amplitudes, 0.1 and 0.8V. A one bit quantizer is used.

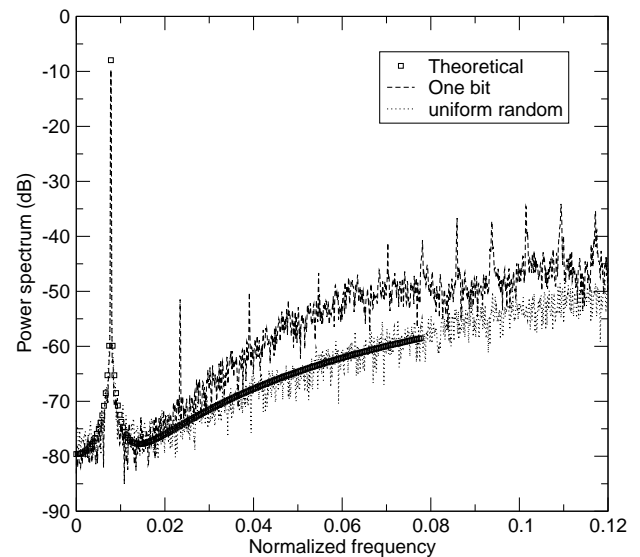


Fig. 6. Output spectrum of a second order modulator with an OSR of 32 and 1% long term clock jitter.

If the output spectrum has a strong harmonic content, the true spectrum differs from the spectrum obtained using the linear model, even if there is no jitter. This deviation is typically not very significant within the signal band. Since the jitter analysis is also done using the linear model, one would

expect some differences from theoretical estimates. This is seen in Figure 6. However, as can be seen from the figure, the match with behavioural simulations is still very good within the signal band. This was found to be true in all the cases simulated, down to an OSR of 16. It is seen from Figure 6 that the theoretical results match well with behavioural simulations if a linear quantizer model is used. The two results also match very well if a two-bit quantizer is used.

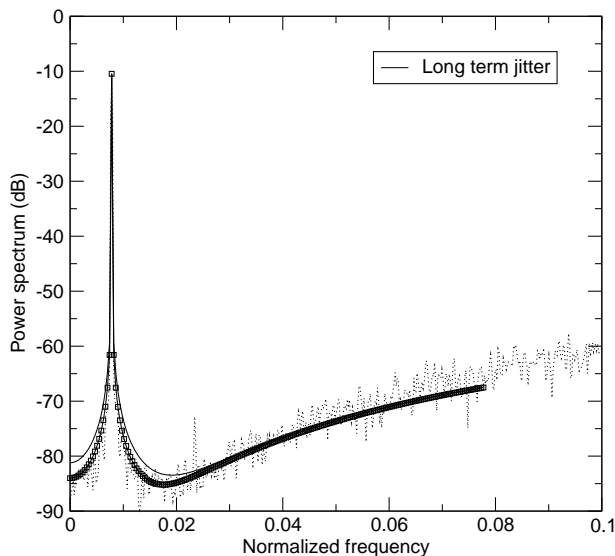


Fig. 7. Output spectrum of a second order modulator with an OSR of 32 and 1% clock jitter. The jitter is a combination of synchronous and long-term jitter. For reference, results for long-term jitter alone is included. A two bit quantizer is used.

It is also possible to use this analysis when the total jitter is a combination of various types of jitter. For example, at the output of the PLL, the total jitter is a combination of synchronous and long-term jitter [1], [2]. Figure 7 shows the results obtained if a combination of long-term jitter and correlated synchronous jitter is used. In this simulation, half the jitter variance is due to synchronous correlated jitter. For reference, the spectrum for long-term jitter alone is also included. It clearly shows there is a reduction in the jitter error (as expected). The Lorentzian spread is also reduced.

In the case of long-term jitter, the additive jitter model itself is not as good an approximation as for the synchronous jitter case. Even here, the match is generally very good up to about $f_s/10$ and always very good up to the Nyquist frequency.

VII. CONCLUSION

In this paper, we have presented a framework to analyze clock jitter in continuous time sigma-delta modulators. The analysis was done for synchronous as well as long-term jitter. The results obtained using the analytical expressions were found to match very well with behavioural simulations. Using the same framework, we have shown that it is possible to obtain the output spectrum, when the clock jitter is a combination of synchronous and long-term jitter. This is typically what would be obtained at the output of the PLL. These analytical expressions are especially useful when jitter variances are

small. In this case, the number of points required to resolve the jitter in behavioural simulations becomes very large.

In this paper, we continue to use the discrete-time model of the modulator. This works well for typical OSRs used. However, a better model would be to have the sampling done after the loop filter.

ACKNOWLEDGEMENT

The author thanks anonymous reviewer 3 for comments that led to better approximations in the analysis and reviewer 1 for comments for improvement in the presentation of the paper.

REFERENCES

- [1] K.Kundert, "Predicting the phase noise of PLL-Based frequency synthesizers," www.designers-guide.com, Nov. 2003.
- [2] A.Mehrotra, "Noise analysis of phase-locked loops," *IEEE Trans. Circuits Syst.-I*, vol. 49, pp. 1309–1316, Sept. 2002.
- [3] J.A.Cherry and W.M.Snelgrove, "Clock jitter and quantizer metastability in continuous-time delta-sigma modulators," *IEEE Trans. Circuits Syst.-II*, vol. 46, pp. 661–676, June 1999.
- [4] H.Tao,L.Toth and J.M.Khoury, "Analysis of timing jitter in bandpass sigma-delta modulators," *IEEE Trans. Circuits Syst.-II*, vol. 46, pp. 991–1001, Aug. 1999.
- [5] O.Oliaei, "State-space analysis of clock jitter in continuous-time oversampling data converters," *IEEE Trans. Circuits Syst.-II*, vol. 50, pp. 31–37, Jan. 2003.
- [6] K.Doris et al., "A general analysis of timing jitter in D/A converters," in *Proc. IEEE ISCAS*, pp. 117–120, 2002.
- [7] Y.Chang et al., "An analytical approach for quantifying clock jitter effects in continuous-time sigma-delta modulator," *IEEE Trans. Circuits Syst.-I*, vol. 53, pp. 1861–68, Sept. 2006.
- [8] W.M.Brown and C.J.Palermo, "System performance in the presence of stochastic delays," *IEEE Trans. Info. theory*, vol. 8, pp. 206–214, Sept. 1962.
- [9] K.F.Riley, M.P.Hobson and S.J.Bence, *Mathematical methods for Physics and Engineering*. Cambridge University Press, 1997.
- [10] N.J.Kasdin, "Discrete simulations of colored noise and stochastic processes and $1/f^\alpha$ power law noise generation," *Proc. IEEE*, vol. 83, pp. 802–827, May 1995.
- [11] A.V.Balakrishnan, "On the problem of time jitter in sampling," *IRE Transactions on Information Theory*, pp. 226–236, April 1962.
- [12] V.Vasudevan, "Simulation of the effects of timing jitter in track-and-hold and sample-and-hold circuits," in *Proc. 42nd Design Automation Conf.*, pp. pp 397–402, 2005.